Interactions between fatty acids and α-synuclein

Christian Lücke,[1] Donald L. Gantz, Elena Klimtchuk, and James A. Hamilton[2]

Department of Physiology and Biophysics, Boston University School of Medicine, Boston, MA 02118

Abstract **α-Synuclein (αS) is an amyloidogenic neuronal protein associated with several neurodegenerative disorders. Although unstructured in solution, αS forms α-helices in the presence of negatively charged lipid surfaces. Moreover, αS was shown to interact with FAs in a manner that promotes protein aggregation. Here, we investigate whether αS has specific FA binding site(s) similar to fatty acid binding proteins (FABPs), such as the intracellular FABPs. Our NMR experiments reveal that FA addition results in *i*) the simultaneous loss of αS signal in both ^{1}H and ^{13}C spectra and *ii*) the appearance of a very broad FA ^{13}C-carboxyl signal. These data exclude high-affinity binding of FA molecules to specific αS sites, as in FABPs. One possible mode of binding was revealed by electron microscopy studies of oleic acid bilayers at pH 7.8; these high-molecular-weight FA aggregates possess a net negative surface charge because they contain FA anions, and they were easily disrupted to form smaller particles in the presence of αS, indicating a direct protein-lipid interaction. We conclude that αS is not likely to act as an intracellular FA carrier. Binding to negatively charged membranes, however, appears to be an intrinsic property of αS that is most likely related to its physiological role(s) in the cell.**—Lücke, C., D. L. Gantz, E. Klimtchuk, and J. A. Hamilton. **Interactions between fatty acids and α-synuclein.** ***J. Lipid Res.*** **2006.** 47: **1714–1724.**

Supplementary key words multidimensional nuclear magnetic resonance spectroscopy • electron microscopy • fatty acid binding • protein-lipid complexes • neurodegenerative disorder

α-Synuclein (αS), a 140 residue cytosolic protein that is water-soluble in its native state, represents in fibrillar form the most abundant protein component of the characteristic Lewy bodies, the pathological hallmark of Parkinson's disease. Despite the pathogenic features associated with misfolded αS, its physiological structure and function have not been resolved to date.

αS is ubiquitously found in the brain, constituting ~1% of the total brain protein content (1). It is localized in part to presynaptic terminals (2), where it loosely associates with synaptic vesicles (3). Several very rare missense mutations of αS (A53T, A30P, and E46K) have been observed in families with autosomal dominant, early-onset forms of Parkinson's disease (4–6). Moreover, triplication of the αS gene was recently discovered in two different families with Parkinson's disease of rather typical onset (7, 8). In the vast majority of cases, however, the wild-type form of the protein is implicated in the development of Lewy body-related abnormalities (9).

Protein misfolding and aggregation are increasingly recognized as the basis for numerous previously idiopathic neurodegenerative diseases in the aged population (10). For example, several intriguing parallels have been reported between the intraneuronal Lewy body deposits of αS in Parkinson's disease and the extracellular amyloid plaques of amyloid β-protein (Aβ) in Alzheimer's disease (11). Moreover, the non-Aβ component (NAC) of amyloid plaque found in the brains of Alzheimer patients turned out to be identical to a 35 residue peptide segment within the αS sequence (12).

One approach toward understanding the role of neuronal proteins such as αS in the pathogenesis of human neurodegenerative diseases is to study their structural organization at the various stages of fibrillization (13) and inclusion formation. A better understanding of the molecular basis of amyloidogenesis could lead to rational therapies that suppress the formation of Lewy bodies and other neurotoxic inclusions. It has been proposed that the accumulation of partially or fully soluble oligomeric forms of αS (some of which have been referred to as protofibrils), rather than the occurrence of mature amyloid fibrils, may be the principal pathogenic event responsible for neuronal dysfunction (14). In the example of Alzheimer's disease, there is evidence that soluble Aβ oligomers can interfere with synaptic efficacy in the absence of protofibrils or fibrils (15).

Although the pathological formation of β-pleated sheet structures in amyloid fibrils is well documented, the physiological conformation(s) and function(s) of αS are still unresolved. In dilute aqueous solution, αS appears to

Manuscript received 3 January 2006 and in revised form 3 May 2006.

Published, JLR Papers in Press, May 10, 2006.
DOI 10.1194/jlr.M600003-JLR200

Abbreviations: Aβ, amyloid β-protein; αS, α-synuclein; DHA, docosahexaenoic acid (22:6 $\Delta^{4,7,10,13,16,19}$); EM, electron microscopy; (I-) FABP, (intestinal) fatty acid binding protein; LA, linolenic acid (18:3 $\Delta^{9,12,15}$); NAC, non-amyloid β-protein component; OA, oleic acid (18:1 Δ^{9}); PLA_2, phospholipase A_2; TOCSY, total correlation spectroscopy; 1D, one-dimensional; 2D, two-dimensional.

[1] Present address of C. Lücke: Max Planck Research Unit for Enzymology of Protein Folding, Weinbergweg 22, D-06120 Halle, Germany.
[2] To whom correspondence should be addressed.
e-mail: jhamilt@bu.edu

be largely unfolded (16), whereas interactions with phospholipid vesicles or detergent micelles appear to induce a highly helical conformational state of the lipid-bound protein (17, 18). Various biophysical studies have reported a supposed preference of αS binding to *i*) unilamellar phospholipid vesicles, *ii*) smaller vesicles with highly curved surfaces, *iii*) negatively charged phospholipid surfaces, *iv*) lipids with long polyunsaturated acyl chains as tail groups, *v*) phospholipids with inositol as the head group, *vi*) phospholipid membranes containing lipid raft-like combinations of oleic acid (OA; 18:1 Δ^9) and PUFA chains, and *vii*) defect structures in the membrane-water interface (17, 19–23). Furthermore, one of these studies indicated a tendency of the αS molecules to oligomerize upon in vitro exposure to bilayer vesicles consisting of phospholipids with only polyunsaturated acyl chains (21). Moreover, the association of αS with biological membranes has been linked to protection of the protein from oxidation or nitration, leading to a reduction of pathological fibrillization (24). Most of these studies, however, did not explain the postulated lipid binding behavior of αS on a molecular basis.

In this study, we analyzed in vitro the interactions of purified αS with several different monounsaturated and polyunsaturated fatty acids using high-resolution NMR spectroscopy and electron microscopy (EM), as previous studies (25–27) had indicated mutual effects that were dependent on the αS and FA concentrations, both in vitro and in vivo. Initially, in vitro measurements of binding interactions between αS and unesterified FAs that were based on the Lipidex assay (25) had led to discussion about a possible relationship to intracellular fatty acid binding proteins (FABPs), a family of cytosolic lipid carriers with a very characteristic β-barrel structure (28). Recent titration microcalorimetry data, on the other hand, did not reveal any specific binding of single FA molecules, either saturated or monounsaturated, to αS (29), as typically observed for FABPs. Moreover, other experiments had demonstrated that, unlike FABPs, the levels of soluble αS oligomers in the cytoplasm are directly affected by FAs (26): PUFAs enhanced the formation of αS oligomers in living mesencephalic neuronal cells, whereas saturated FAs inhibited their formation; both effects were replicated in vitro using purified recombinant αS. As a consequence, we set out to compare αS with FABPs, because the interaction of αS with FAs is apparently of major physiological significance for the role of αS inside the cell. For example, an association between αS oligomer accumulation and altered FA composition was found in the brains of patients with certain synucleinopathies (27). More precisely, specific long-chain PUFA levels were increased in the soluble brain fraction of patients with either Parkinson's disease or a related disorder, Lewy body dementia, compared with normal age-matched subjects. Similarly, altered FA compositions were detected in cells that either overexpress or entirely lack αS, in contrast with the normal cells (27). Just recently, a disruption of FA uptake and trafficking was observed in vivo in astrocytes from αS gene-ablated mice (30).

With protocols designed to detect specific interactions between a particular protein and individual FA molecules by the use of NMR, we explored whether αS has high-affinity FA binding sites, similar to those revealed for FABPs and serum albumin via the same method (28, 31). Instead, however, the NMR data indicated the formation of high-molecular-weight FA-αS complexes. Subsequently, EM was used to visualize the morphology of these biomolecular aggregates.

MATERIALS AND METHODS

All nonlabeled FAs were obtained from Sigma (St. Louis, MO); [1-^{13}C]OA was acquired from Cambridge Isotope Laboratories (Andover, MA). Deuterated water [^2H_2O; ^{2}H 99.9%] was purchased from Wilmad (Buena, NJ). All other chemicals used were of analytical grade.

Rat intestinal (I-)FABP was prepared as described previously (32), with the exception that a Hi-Load Superdex G-75 column (60 cm × 1.6 cm), equilibrated with 50 mM sodium phosphate buffer, 300 mM NaCl, and 0.05% sodium azide at pH 7.8, was used for size exclusion.

Purified human αS, which was kindly provided by Ronit Sharon (Brigham and Women's Hospital, Boston, MA), had been prepared as described previously (16, 33). Gas chromatographic analysis showed that the protein was free of endogenous FA. For molecular weight determinations, αS protein samples (2 μg) were applied on precast SDS gels (Tris-glycine, 8–16% acrylamide gradient) from Bio-Rad and subsequently subjected to Western blot analysis using LB509 (Chemicon, Temecula, CA) as anti-αS antibody. The relative band migrations were analyzed with a standard BenchMark prestained protein ladder (Invitrogen, Carlsbad, CA) using AlphaEase 5.5 software (Alpha Innotech Corp., San Leandro, CA).

Before each NMR and EM experiment, αS samples were prepared fresh from the lyophilized material that was filtered through Microcon concentrators with a 100 kDa cutoff (Millipore, Billerica, MA) to remove protein aggregates. The FAs were added as sodium or potassium salts from concentrated stock solutions (34).

NMR experiments

A Bruker (Rheinstetten, Germany) AVANCE 500 MHz spectrometer, equipped with a 5 mm inverse triple-resonance probe that has XYZ-gradient capability, was used to carry out all NMR experiments. All NMR spectra were collected at 25°C in a phase-sensitive mode, implementing time-proportional phase incrementation for quadrature detection. The ^{1}H and ^{13}C chemical shift values were referenced to external 2,2-dimethyl-2-silapentane-5-sulfonate (Cambridge Isotope Laboratories). In the one-dimensional (1D) and two-dimensional (2D) ^{1}H experiments, the water signal (H_2O/D_2O ratio of 95:5) was suppressed by selective presaturation during the relaxation delay (1.3 s), with the carrier placed in the center of the spectrum on the water resonance. 1D ^{1}H data (128 scans, 4 k time domain size) were collected with 7,507.5 Hz (15 ppm) spectral width. For shorter data collection during the titration experiments, the 2D ^{1}H/^{1}H-total correlation spectroscopy (TOCSY; spinlock time of 75 ms) and 2D ^{1}H/^{1}H-NOESY (mixing time of 150 ms) spectra were acquired with 7,507.5 Hz spectral width in both time domains, but only eight scans and 2,048 × 256 data points. Regular 2D data sets, on the other hand, were collected with 64 scans and 2,048 × 512 data points. For the 1D ^{13}C experiments of αS (30,000 scans, 16 k time domain size), a relaxation delay of 2 s and a spectral width of 27,777.8 Hz (221 ppm) was applied. The 1D ^{13}C spectra of I-FABP were collected with 6 k scans, 4 k time domain size, 1 s

relaxation delay, and a spectral width of 28,985.508 Hz (230 ppm). All NMR spectra were acquired, processed, and analyzed using the XWINNMR 2.6 software package (Bruker).

Titrations of αS (1 mM) were performed *i*) in 20 mM potassium phosphate buffer (pH 5.5) with aliquots of 50 mM sodium linolenate, *ii*) in 10 mM Tris buffer (pH 6.0) with aliquots of 50 mM sodium docosahexaenoate, or *iii*) in 10 mM Tris buffer (125 mM NaCl, pH 7.7) with aliquots of 83.3 mM potassium [1-^{13}C]oleate. Titrations of I-FABP (1 mM) were performed in 25 mM sodium phosphate buffer (150 mM NaCl, 0.05% sodium azide, pH 7.4) with aliquots of 83.3 mM potassium [1-^{13}C]oleate to achieve the desired FA/protein molar ratio.

EM experiments

Samples of 200 μl final volume were prepared in 10 mM Tris buffer (125 mM NaCl, pH 7.8) containing *i*) 1 mM OA, *ii*) 1 mM αS, or *iii*) 1 mM OA plus 1 mM αS. The samples were either mixed gently or vortexed for 90 s at maximal power. To visualize the aggregate structures by EM, a modification of the negative staining drop technique (35) was used. Aliquots of 5 μl were incubated for 10 s on carbon- and Formvar-coated, 200 mesh copper grids that had been glow-discharged to promote sample spreading (36). The grids were then rinsed with 10 drops of Millipore-filtered (0.2 μm) water to reduce the salt concentration. After removal of the excess fluid by blotting, the samples were stained for 10 s with 1% sodium phosphotungstate at pH 7.5, blotted again, and air-dried. All images were recorded under low-dose conditions on SO163 film in a CM12 transmission electron microscope (Philips Electron Optics, Eindhoven, The Netherlands).

RESULTS

NMR data

To probe the interactions of FAs with αS at a molecular level, we performed high-resolution NMR experiments at 11.7 T. Homonuclear 1D and 2D spectra of αS in aqueous buffer solution (pH 5.5) were first obtained under conditions typical for NMR-based structural analysis of FABPs (37–39). In this acidic environment, FAs bind to FABPs with high affinity while the exchange of the amide protons is suppressed, thus allowing a better detection of the highly relevant amide proton resonances by NMR. The 2D TOCSY experiments are designed to show short- and long-range ^{1}H couplings through chemical bonds; they form the basis for making rigorous assignments of protein spectra. Both the 1D and 2D NMR spectra of αS without FAs showed a rather low signal dispersion and hence extensive spectral overlap (**Fig. 1**), as is typical for unfolded proteins. Moreover, the ^{1}H resonances of most αS residues displayed standard chemical shift values (in ppm), as usually observed in "random coil" structures. Hence, a quantitative analysis of the protein secondary structure according to Wishart, Sykes, and Richards (40) yielded no significant α-helix or β-sheet percentages based on these 2D NMR spectra. This result is consistent with other NMR data of αS that were derived from a heteronuclear 2D experiment (^{1}H/^{15}N-HSQC) (18) but strikingly different from data obtained for FABP family members, which exhibit extensive secondary and tertiary structure under similar experimental conditions (38, 39).

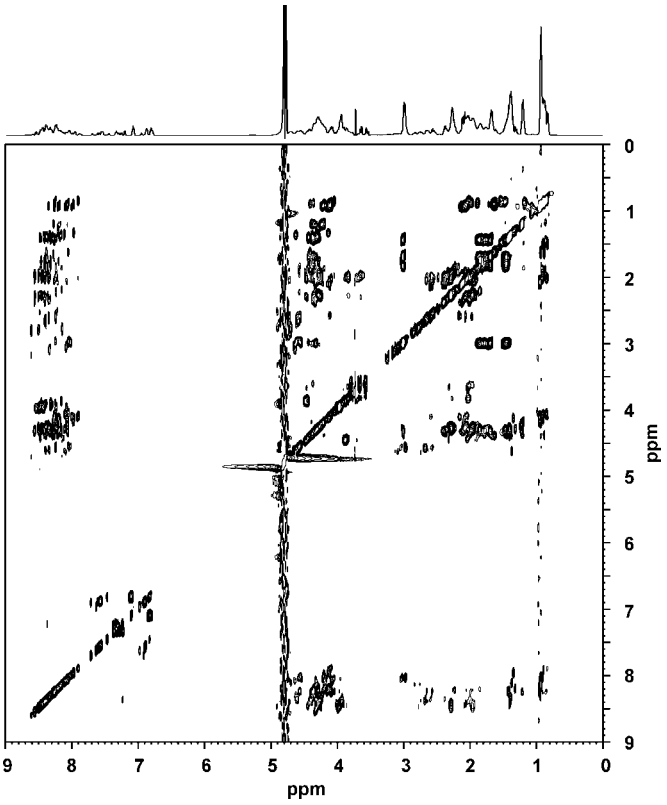

Fig. 1. Two-dimensional (2D) ^{1}H/^{1}H-total correlation spectroscopy (TOCSY) spectrum of 1 mM human α-synuclein (αS) (20 mM potassium phosphate buffer, pH 5.5, 25°C). The signal distributions in the 2D plot and the one-dimensional (1D) trace on top show little signal dispersion for this 14 kDa protein, implying a mostly random coil structure in aqueous solution.

Because of this apparent lack of tertiary structure in water-soluble αS, we did not proceed with the analysis of NOESY spectra (data not shown), which directly reflect atomic distances between ^{1}H nuclei, to derive the solution-state structure of the protein. Instead, we focused on the interactions between αS and different FA species.

We initiated our studies of FA binding to αS with the PUFA linolenic acid (LA; 18:3 $\Delta^{9,12,15}$), because PUFAs have been shown to induce αS oligomerization both in vitro and in vivo (21, 26). The addition of equimolar or higher amounts of LA to a 1 mM αS solution at pH 5.5 produced no chemical shift changes in either the 1D or 2D NMR spectra, which would be indicative of conformational rearrangements within the protein structure. The so-called "fingerprint region" in the 2D ^{1}H/^{1}H-TOCSY spectrum, which exhibits protein signals between the backbone amide and the corresponding C^{α} protons, is particularly sensitive for detecting even small conformational changes. However, the superposed fingerprint regions of two ^{1}H/^{1}H-TOCSY spectra collected *i*) without LA and *ii*) with a 10-fold excess of LA (i.e., final FA concentration = 10 mM) showed no additional or shifted signals in the presence of FAs (**Fig. 2**). Hence, these NMR spectra in solution show that even a large molar excess of FAs causes no discernible changes in the tertiary structure of water-soluble αS. Moreover, the possibility that the protein binds FA

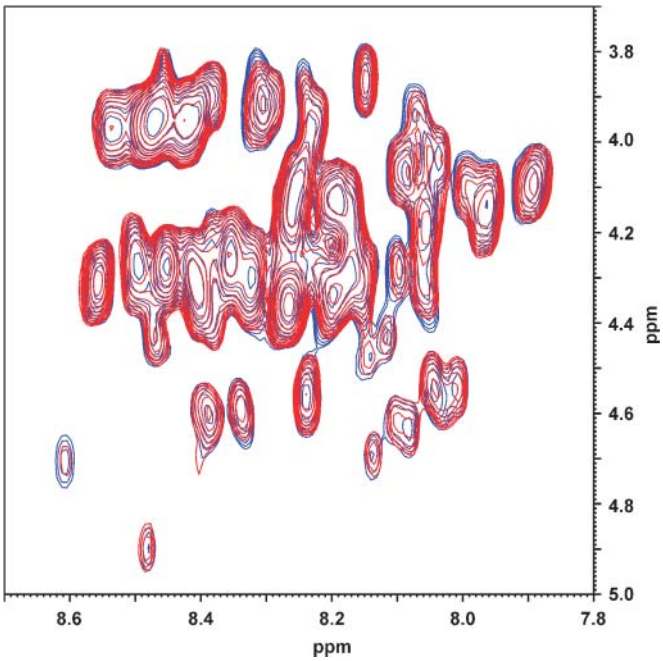

Fig. 2. Fingerprint region from two $^{1}H/^{1}H$-TOCSY spectra of 1 mM human αS in the presence (red) and absence (blue) of a 10-fold linolenic acid (LA; 18:3 $\Delta^{9,12,15}$) excess (20 mM potassium phosphate buffer, pH 5.5, 25°C). No chemical shift (ppm) changes, which would indicate either differences in the conformation of the soluble protein or the presence of discrete high-affinity FA binding sites, were observed upon addition of the FAs.

molecules in discrete high-affinity binding sites, which should produce at least some specific alterations of the local chemical environment inside the binding pocket (as seen with FABPs), is highly unlikely because of the apparent lack of chemical shift changes.

1D ^{1}H-NMR spectra obtained with different FA/αS molar ratios up to 10:1 (**Fig. 3A**) revealed a stepwise decrease of the protein signal intensities with increasing fatty acid concentrations. The corresponding intensity changes upon addition of LA are displayed graphically for two selected αS amide proton peaks in Fig. 3B. αS solutions were also titrated with the PUFA docosahexaenoic acid (DHA; 22:6 $\Delta^{4,7,10,13,16,19}$) at pH 6.0 and with monounsaturated OA at pH 7.7 to cover a wider range of experimental conditions; the spectral results (data not shown), however, were similar to those found for LA. This general decrease in the protein signal intensities with increasing FA ratios implies a reduction of the monomeric αS concentration in solution, even though no concomitant protein precipitate was observed. Moreover, no narrow FA signals, which would indicate a population of single FA molecules bound with high affinity to soluble αS, appeared with increasing FA concentrations. Instead, the results rather suggest that the presence of FAs caused αS to form high-molecular-weight complexes with the lipid, thereby reducing its molecular tumbling rate to the extent that the ^{1}H signals disappeared from the NMR spectrum as a result of excessive line-broadening.

Western blot analysis of the LA-αS mixture at 10:1 ratio, which was obtained from the corresponding NMR sample, revealed the presence of various oligomeric αS forms, whereas the corresponding αS samples lacking FAs displayed only the monomeric protein form (**Fig. 4**). These data, as well as the fact that the decrease of monomeric

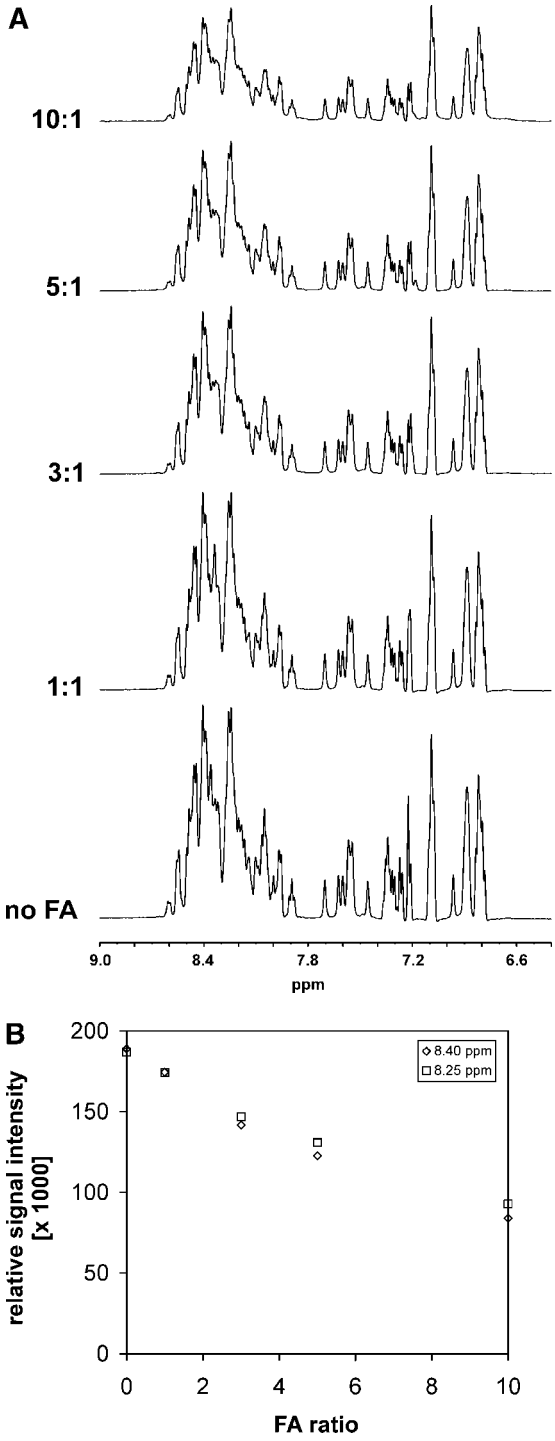

Fig. 3. A: 1D ^{1}H-NMR spectra displaying the amide and aromatic proton region of αS at increasing LA/αS ratios (left margin). The 1 mM protein solution (20 mM potassium phosphate buffer, pH 5.5, 25°C) was titrated with aliquots of 50 mM LA. The decreasing signal intensities indicate a stepwise reduction of the monomeric protein concentration in solution. B: The loss in αS signal intensity upon addition of LA is plotted for two amide proton resonances at 8.40 ppm (diamonds) and 8.25 ppm (squares).

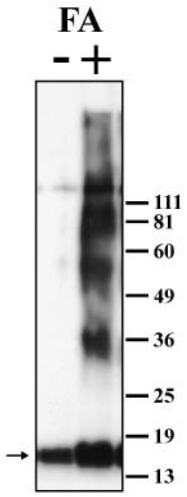

Fig. 4. Western blot of αS in the presence and absence of LA. On this type of gel, monomeric αS (arrow) typically migrates with an apparent molecular mass of ~17 kDa, which is slightly above its true mass of 14 kDa. αS that was not exposed to any FA (left lane) appeared solely in the monomeric form. On the other hand, a LA-αS mixture at a ratio of 10:1 (right lane), which was generated in the NMR titration study depicted in Fig. 3A, clearly shows both monomeric and oligomeric protein forms. Note that the detected amount of αS is overall higher in the presence of FAs, even though identical protein quantities (2 μg per lane) had been applied; this seems to be attributable to FA-induced changes in the protein conformation, which enable improved recognition by the antibody (see Fig. 4 in reference 26). [This figure was kindly provided by Ronit Sharon (Brigham and Women's Hospital, Boston, MA).]

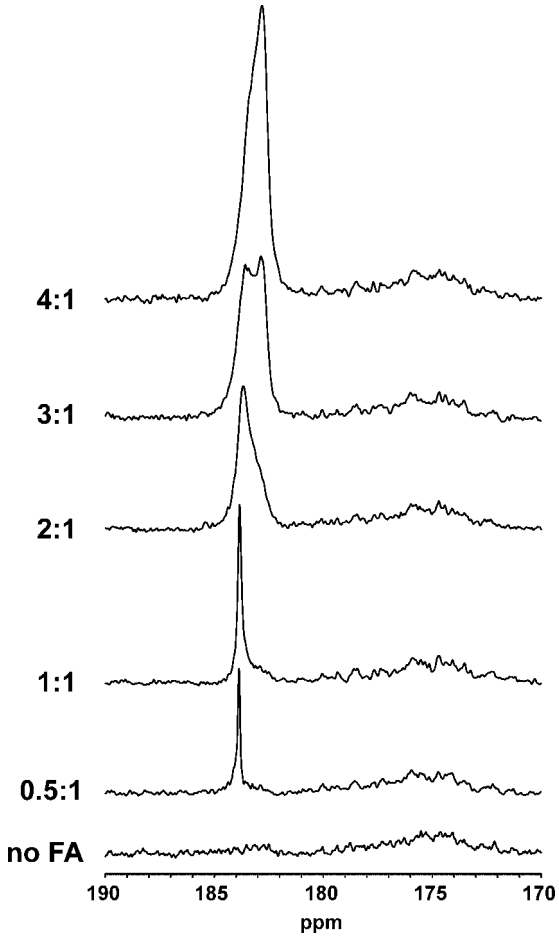

Fig. 5. 1D ^{13}C-NMR spectra showing the carbonyl region of intestinal fatty acid binding protein (I-FABP) at increasing oleic acid (OA; 18:1 Δ^9)/I-FABP ratios (left margin). The 1 mM protein solution (25 mM sodium phosphate buffer, pH 7.4, 25°C) was titrated with aliquots of 83.3 mM 1-^{13}C-labeled OA. The addition of 1-^{13}C-labeled OA up to 1:1 molar ratio produced a very sharp signal (~30 Hz half-width) at 183.8 ppm, which represents OA bound to the single FA binding site in I-FABP. Further addition of OA caused a second, ~4-fold broader peak to appear at 182.8 ppm, as the excess unbound FA started to form aggregates. The protein-derived carbonyl signals between 171 and 181 ppm remained basically unaltered.

αS concentration in the NMR solutions is induced entirely by the addition of FA, suggest that the resulting high-molecular-weight complexes consist not solely of protein but also include lipid. Moreover, our NMR spectra do not support the existence of soluble αS dimers, whose molecular mass (28 kDa) is still far enough below the size limit at which excessive line-broadening would render signal detection impossible. Hence, assuming that the highly concentrated NMR sample we used consisted solely of high-molecular-weight FA-αS aggregates, the fairly large amount of αS dimer species observed on the Western blot may be the result of a reversible decomposition into smaller oligomer fragments as a result of FA loss on the gel or during gel preparation.

To define more precisely the physical state of the FAs in the aqueous buffer solutions used here, we next used ^{13}C-NMR and EM. ^{13}C-NMR spectroscopy with ^{13}C-carboxyl-labeled FAs is a very sensitive and specific method for the detection of FAs bound to individual protein binding sites, as demonstrated previously in studies of intracellular FABPs and serum albumin (41, 42). We now performed ^{13}C-NMR binding studies with nonlabeled rat I-FABP for direct comparison with αS. As shown in **Fig. 5**, the carbonyl resonances of I-FABP at natural ^{13}C abundance are near the noise level of the 1D ^{13}C-NMR spectra. With the addition of small amounts of 1-^{13}C-labeled OA at pH 7.4, a narrow signal (~30 Hz half-width) appears at 183.8 ppm. This peak represents a single OA molecule bound to I-FABP (41), because *i*) the concentration of unbound FA monomers in aqueous solution is too low to be detected by NMR and *ii*) high-molecular-weight FA complexes exhibit broader line shapes as a result of reduced molecular tumbling rates. The addition of OA above a FA/protein ratio of 1:1 resulted in the appearance of a second, ~4-fold broader peak at 182.8 ppm, whereas the protein signal intensities remained the same. This new peak apparently derives from the excess FA molecules that could not bind to I-FABP above an equimolar ratio but rather formed high-molecular-weight lipid aggregates instead. The intensity of the signal at 183.8 ppm, which represents the FA-FABP complex, was not affected by the further increase of FA concentration beyond the 1:1 molar ratio.

In contrast, the 1D carbon NMR spectra of αS (**Fig. 6**), obtained with increasing amounts of 1-^{13}C-labeled OA, exhibited the following differences compared with I-FABP.

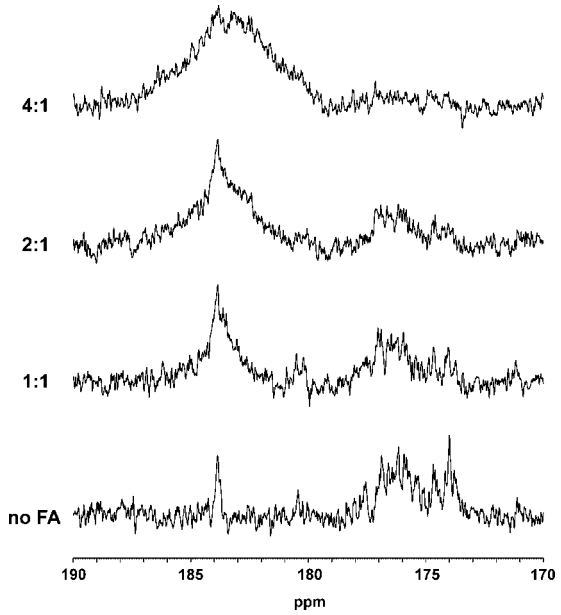

Fig. 6. 1D ^{13}C-NMR spectra showing the carbonyl region of αS at increasing OA/αS ratios (left margin). The 1 mM protein solution (10 mM Tris buffer, pH 7.7, 25°C) was titrated with aliquots of 83.3 mM 1-^{13}C-labeled OA. The decreasing signal intensities of the protein backbone and side chain carbonyls between 171 and 181 ppm indicate a stepwise reduction of the protein monomer concentration in solution (the narrow peak at 183.9 ppm derives from the side chain carboxyl resonances of the 18 glutamate residues in αS). At the same time, the continuous increase of the extremely broad peak (~470 Hz half-width) at ~183 ppm with increasing FA/αS ratios can be attributed to the appearance of high-molecular-weight lipid aggregates that seem to be considerably larger than those formed in the presence of I-FABP (see Fig. 5).

First, the carbon signals of the nonlabeled protein showed progressively decreasing signal intensities. This intensity decrease, which is analogous to the above-described ^{1}H-NMR results, was observed not only for the carbonyl resonances displayed in Fig. 6 but also for all other carbon resonances of αS (data not shown). A second significant difference in these ^{13}C spectra was that the carbon signal originating from the OA ^{13}C-carboxyl group turned out to be considerably broader (~470 Hz half-width) than the FA peaks that appeared in the OA titration of I-FABP, indicating a yet higher aggregate weight of the FA complex forms, probably because of the incorporation of αS molecules. This broad signal emerged at ~183 ppm, next to a narrow peak at 183.9 ppm that derives from the side chain carboxyl groups of the 18 glutamate residues present in the αS sequence (**Table 1**).

Hence, these NMR data obtained upon the addition of OA to αS differ markedly from previous results (28, 31) when OA was added to FABP or albumin at comparable protein and FA concentrations (i.e., 1–2 mM protein in the presence of equimolar amounts or stoichiometric excess of ligand), as demonstrated here with I-FABP. First, the protein signals of FABP (and albumin) show no intensity changes with the addition of FA; that is, these proteins remain in solution without aggregation or oligomerization. In the case of αS, on the other hand, the protein signals diminished progressively with increasing FA concentration, both in the ^{1}H and ^{13}C spectra. Second, the ^{1}H signals of residues located in the high-affinity binding site(s) of FABP family members usually display significant chemical shift changes in the presence of FAs owing to the immediate vicinity of the bound ligand (37). In the ^{1}H spectra of αS, however, no soluble protein state other than the monomeric apo form is observed. Finally, the OA carboxyl group yields a single narrow peak when bound to FABP (or a cluster of narrow peaks representing several discrete binding sites when bound to albumin), because the segmental motions of the FAs within the binding site(s) are fast compared with the aggregated FA state (43); the intensities of these narrow peaks increase until all protein sites are filled (1 site in I-FABP, 2 sites in liver FABP, and ~10 sites in albumin), whereas an additional, broader OA carboxyl peak appears only after saturation of all high-affinity binding sites (34, 44). Yet, the significantly broader OA carboxyl peak observed in the αS spectra only provides evidence for a high-molecular-weight aggregate state of the FAs. This aggregate state cannot be micellar, because micelles *i*) usually occur only above pH 9 and *ii*) generally display narrow line widths in the ^{13}C-NMR spectra (45), in accordance with a loosely structured aggregate of ~8.4 kDa calculated mass. Rather, the FA aggregates observed with αS must be considerably larger to cause the extreme line-broadening effects observed in the NMR spectra. Moreover, narrow FA signals, as would be expected for a water-soluble protein with high-affinity FA binding site(s), did not emerge in the ^{13}C spectra of αS upon the addition of equimolar OA amounts, although under these conditions monomeric αS apparently remains in solution in sufficient quantities (Fig. 3A) to generally permit the binding of single FA molecules from the surrounding medium. These molecules would be derived from the FA pool, either as free FAs that exist in nanomolar to micromolar concentrations in aqueous solution (46) or as FAs bound in high-molecular-weight aggregates, such as acid-soap bilayers when the pH is near neutrality (45).

EM data

In an attempt to visualize and structurally characterize the FA aggregate forms that we have postulated from the

TABLE 1. Amino acid sequence of human α-synuclein

1	M*D*V**K**GLS**K**A**K***E*GVVAAA*E***K**T**K**Q*E*VA*E*AAG**K**T**K***E*GVLYVGS**K**T**K***E*GVVH
51	GVATVA*E***K**T**K***E*QVTNVGGAVVTGVTAVAQ**K**T*V**E*GAGSIAAATGFV**KK***D*QL
101	G**K**N*EE*GAPQ*E*GIL*ED*MPV*DP**D**NEAY*E*MPS*EE*GYQ*D*Y*E*PEA

The seven imperfectly repeated hexamer motifs are underlined. Acidic and basic residues are indicated in italic and boldface type, respectively.

indirect NMR evidence, we used negative stain EM. To this end, we examined samples prepared under identical conditions as the above-described ^{13}C-NMR experiments.

First, samples containing 1 mM OA (pH 7.8) were investigated without any protein present to characterize their general appearance. The images revealed large, electron-lucent spherical objects up to 160 nm in diameter (the dark halo around these particles is indicative of stain buildup) as well as smaller tapered objects of ~70 × 35 nm (**Fig. 7A, B**). It can be concluded that these heterogeneously sized objects all represent FA aggregates, because *i*) the micrographs showed characteristics of lipids, which typically exclude stain (47), and *ii*) samples containing higher OA concentrations displayed increased numbers of such objects (data not shown). The particle size and shape in OA preparations that had been gently mixed (Fig. 7A) were very similar to those in preparations vortexed vigorously for 90 s (Fig. 7B). At the selected conditions (1 mM OA, pH 7.8, and 25°C), FAs are predicted to consist predominantly of a lamellar FA-soap phase (45), as discussed in detail below. Thus, the large particles in our EM images are most likely multilamellar structures. Their bilayer structure, however, was not visualized, and the membrane thickness could not be determined, because the phosphotungstate stain did not penetrate the negatively charged lipid surfaces to enter the cores of the particles.

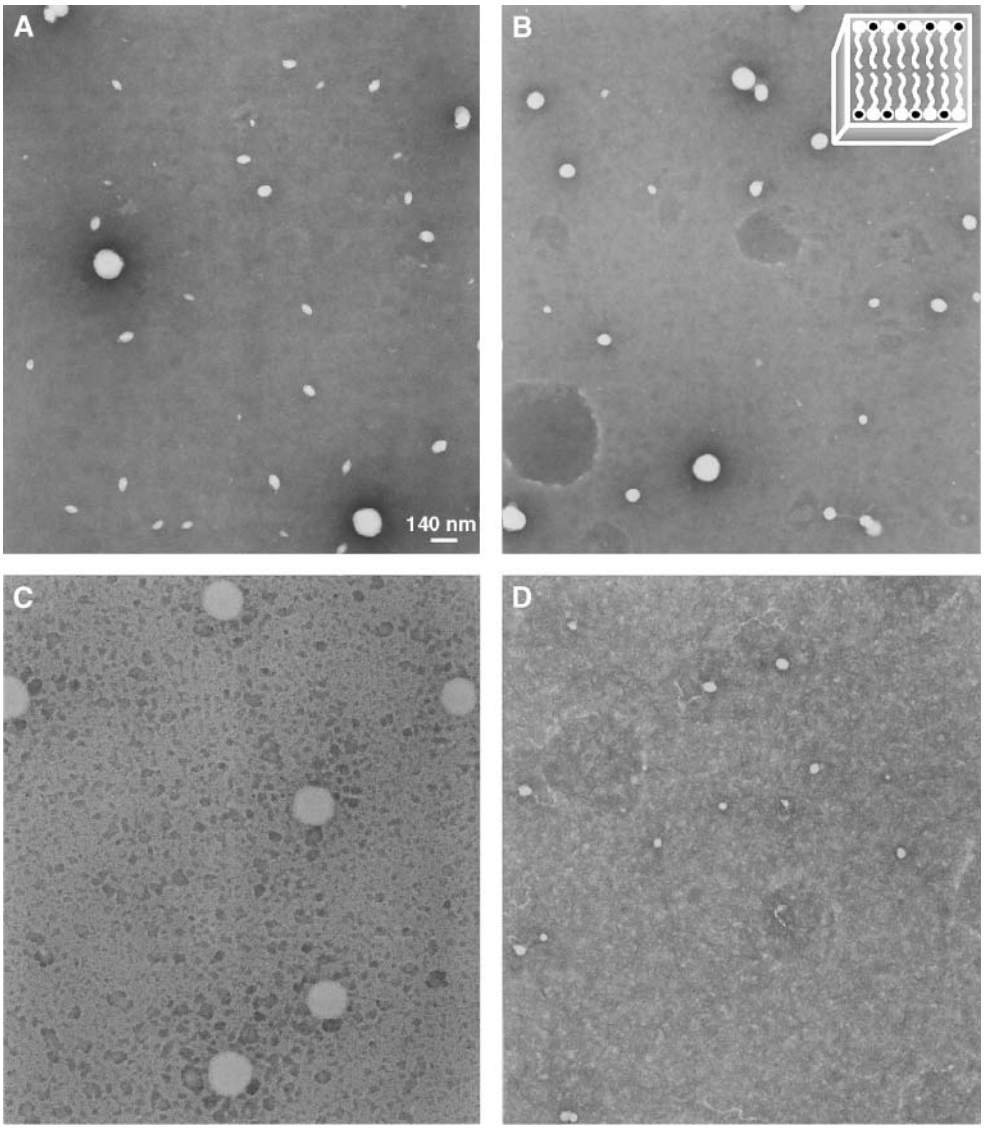

Fig. 7. Electron micrographs of 1 mM OA in the absence (A, B) and presence (C, D) of 1 mM αS. The protein-free solutions looked very similar both without (A) and with (B) vortexing, displaying large spherical and smaller tapered objects. In the presence of αS, these lipid particles appeared slightly larger and more electron-dense as long as no additional energy input was applied (C). Upon vortexing, however, an extensive disruption of the lipid particles was observed (D). Original images were taken at 70,000-fold magnification; white bar in A = 140 nm. The schematic drawing in the upper right corner of B represents a FA-soap bilayer structure (45), in which approximately half of the carboxylate head groups are uncharged (i.e., protonated) and the other half are negatively charged (i.e., deprotonated), as indicated by circles filled in white and black, respectively.

If we assume that these structures consist entirely of FA molecules without any water inside, the calculated aggregate weight of the spherical and tapered particles ($\sim 2 \times 10^6$ and 62×10^3 kDa, respectively) is much too large to yield observable NMR signals. And even if the observed structures were monolamellar vesicles consisting of only a single bilayer (Fig. 7B, inset), the aggregate weights of the two different particle forms (313×10^3 and 28×10^3 kDa, respectively, not including the enclosed water molecules) would still cause excessive line-broadening in the NMR spectra because of very slow tumbling rates.

When αS was added to OA at a 1:1 molar ratio (i.e., a large excess of protein molecules relative to the number of lipid particles), spherical particles up to 230 nm in diameter were present after gentle mixing (Fig. 7C). These particles were more electron-dense and larger in diameter than those in Fig. 7A. We assume that the overall positively charged N-terminal domain of αS (Table 1) attaches to the negatively charged surface of an OA aggregate. Hence, the increased electron-density of the OA-αS complex is at least in part attributable to αS located on the particle surface. For comparison, 1 mM αS with no FAs present, prepared under identical negative staining conditions, contained only thin, slightly electron-lucent strands surrounded by denser stain (data not shown).

Additional evidence for an interaction between αS and the FA aggregate structures is illustrated in Fig. 7D. The large FA particles, which were observed at an OA/αS ratio of 1:1 after gentle mixing (Fig. 7C), were disrupted by the vortexing procedure, leading exclusively to smaller particles (~30–70 nm in diameter; Fig. 7D). This particle disruption provides strong evidence that the presence of αS destabilizes the OA aggregates, because vigorous vortexing did not disrupt the protein-free lipid particles (compare Fig. 7B versus 7A).

Similar observations were reported by two recent studies in which soluble monomeric αS caused the disruption of membranes composed of phospholipid bilayers (20, 48). Destabilization of the OA particles by αS might furthermore explain why the OA-αS aggregates in Fig. 7C appear larger than the protein-free OA aggregates in Fig. 7A, as a flattening of αS-laden particles that adhere to the carbon surface could possibly produce an increase in diameter accompanied by a (nondetectable) reduction in height.

It must be noted that our EM study cannot necessarily be extrapolated to the acidic pH conditions used in some of our NMR experiments. Below neutral pH, the acid-soap bilayer begins to accommodate the uncharged FAs until it eventually undergoes a phase change to an unstructured oil phase. The NMR results showing a decrease of the soluble protein concentration at pH 5.5 and 6.0 upon the addition of LA and DHA, respectively, therefore could reflect either the binding of αS to remnant acid-soap structures or a different mode of binding than that observed above neutral pH.

DISCUSSION

The synucleins are highly conserved neuronal proteins (9); the amino acid sequence of human αS is shown in Table 1. The N-terminal region of αS (residues 1–60) contains most of the basic residues (i.e., 11 of 15 lysines, without any arginines present), with a recurring 11 residue sequence that includes seven imperfectly repeated hexamer (KTKEGV) motifs. This region is very similar in all three members of the synuclein family (α-, β-, and γ-synucleins). The central part of the αS sequence (residues 61–95) comprises the highly hydrophobic NAC domain, which by itself can readily form amyloid fibrils under physiological conditions (3); partial deletion of the NAC region in β-synuclein made this protein nonamyloidogenic. Finally, the less conserved C-terminal region of αS (residues 96–140) is characterized by a high content of acidic residues (two-thirds of all aspartate and glutamate residues occur in the last one-third of the protein sequence).

Although purified αS exists in a nearly completely unfolded state in aqueous solution, most structural studies of αS suggest a predominantly helical secondary structure in the presence of lipid membranes (17, 18, 49, 50). The circular dichroism study of Davidson and coworkers (17) demonstrated that the helicity of water-soluble monomeric αS increases drastically from a negligible amount (~3%) up to 82% in the presence of unilamellar phospholipid vesicles. Moreover, the protein preferentially associates with small unilamellar vesicles that contain acidic phospholipids (net negative charge), whereas no binding was observed to vesicles with a net neutral charge. Based on these data, structural models have been developed that feature helices in which the positively charged lysine side chains are generally located at the water-lipid interface (17, 49, 50). Recently, NMR data have shown that the N-terminus of αS folds in the presence of SDS micelles into two approximately equally long helices (49–51). Only this net positively charged domain spanning residues 1–102 is involved in binding to the lipid surface, whereas the C-terminal end with net negative charge remains unaffected and freely mobile in solution.

In this study, we raised the question about the type of interaction that occurs between αS and FAs. Based on the close similarity in the molecular weights of FABPs and αS, and because of some correspondence in the amino acid sequences, it has previously been suggested that αS might be a member of the intracellular FABP family (25). However, there are several notable differences. FABPs *i*) have a well-defined tertiary structure with a high β-sheet content in solution; therefore, they *ii*) exhibit a high ^{1}H-NMR signal dispersion both in the absence and presence of FAs and *iii*) remain monomeric and structurally unchanged in solution in the presence of excess FAs. They also bind maximally one to two FA molecules per protein in specific binding sites and thus reveal narrow carboxyl signal line width(s) for bound FAs. As none of these features apply to purified αS, we conclude that αS is not a member of the FABP family. Moreover, the binding properties of αS do not resemble those of other known high-affinity FA binding proteins (31), including the highly α-helical serum albumin.

Nevertheless, our results support the general hypothesis that αS preferentially binds to negatively charged surfaces. At millimolar concentrations and over a range of several

pH values centered at neutral pH, long-chain FAs are well above their solubility limit and tend to aggregate (45, 52). At room temperature, OA forms either an oil phase at low pH or a lamellar acid-soap bilayer near neutrality. As we did not observe any phase separation at pH 5.5 or 6.0, the physical state of the FAs in those experiments is not clear. However, an interaction of αS with the FA phase was obvious from the changes in αS signal intensity that were observed. Hence, even at pH 5.5, the FAs apparently produced an environment suitable for the formation of αS-FA aggregates. In the case of the experiments performed at pH $>$ 7, however, the FA aggregates definitely have a lamellar bilayer structure. These acid-soap bilayers (Fig. 7B, inset), which are similar to phospholipid bilayers in their molecular organization, are composed of both unionized (uncharged) and ionized (negatively charged) FAs, thus creating a net negative charge at the bilayer surface that could serve as a docking site for αS molecules. A recent study by Chen and Szostak (53) has shown that at pH 8.5 OA tends to aggregate, first forming small micelles, then medium sized intermediates with an average hydrodynamic radius of 45 nm, and finally, after a period of several hours, bilayered vesicles of 130 nm radius. Binding of more than one αS molecule to such aggregate structures could account for the previously reported in vitro appearance of αS oligomeric forms in the presence of high FA concentrations (21, 26). It should be noted, however, that αS oligomerization has also been observed at lower FA concentrations near the solubility limit (26), at which no lipid aggregate structures could be detected by light scattering (Ronit Sharon, personal communication). Apparently, even a few FA molecules may provide the necessary lipid nucleus that is required for protein oligomerization to occur.

Of course, we cannot completely rule out low-affinity FA binding to αS monomers or oligomers in solution if this interaction is so weak that it causes no concomitant conformational changes in the protein. The strong propensity of αS to adopt a helical structure in the presence of negatively charged lipid surfaces such as acidic phospholipid bilayers or detergent micelles (17, 19), however, makes this possibility seem very unlikely. In addition, although water-soluble αS dimers or trimers were not observed under the conditions used in our NMR experiments, we cannot exclude the possibility, based on the data presented here, that smaller, biologically active FA-αS complexes could exist in less concentrated solutions. Nevertheless, our data support the formation of high-molecular-weight FA-αS complexes with slowed molecular tumbling rates that result in extensive line-broadening of both the protein and FA signals.

The broadened OA carboxyl signal in the presence of αS further indicates that this particular protein stimulates the formation of yet larger FA aggregate structures compared with those found in the presence of I-FABP. This latter effect was also observed in the EM micrographs of unperturbed OA-αS samples. Upon mechanical agitation in the presence of a high αS concentration, however, the large FA aggregates were broken down into smaller particles. Presumably, the partially immersed helical protein molecules, in particular when αS oligomers are formed, cause a disruption of the lipid surface similar to membranolytic peptides such as melittin. The exact composition(s) of these FA-αS aggregates and the mechanism(s) of their formation will have to be clarified in future studies.

The natural function of αS thus appears to be related to its tendency to adopt a predominantly helical conformation in the presence of (preferably negatively charged) lipid surfaces, such as the biological membranes of various subcellular compartments. This interaction is apparently based on two physical criteria typically found in biological membranes: *i*) a net negative lipid surface charge that presumably interacts with the positively charged N-terminal domain of αS, and *ii*) a hydrophobic, fluid lipid core consisting, for example, of polyunsaturated acyl chains that better allow the protein to immerse into the membrane layer. Other studies have already shown that αS prefers to bind to PUFAs or to PUFA-esterified lipids (21). As the fatty acyl chains of PUFAs are more disordered compared to saturated FAs (54), they should allow a better penetration of the αS side chains below a lipid-composed surface.

How do these in vitro results relate to the brain, where the steady-state concentration of free (unbound) FAs is very low? As in other tissues, most FAs are bound either to cell membranes or to intracellular lipid binding proteins such as FABPs, thus keeping the concentration of unbound FAs in the submicromolar range, well below their solubility limit. The documented presence of FA aggregates within cells is extremely rare and has been associated with severe pathology in peroxisomal disorders, such as X-linked adrenoleukodystrophy (55). Therefore, acid-soap bilayers, as formed in our in vitro studies, are not expected to be present in the cytosol of brain cells to act as catalysts for the adsorption of αS. Rather, αS appears to be attracted to negatively charged membrane surfaces (17, 19).

Nevertheless, FAs could still play a role in the natural function of αS in the brain. Unesterified FAs enter the brain continuously as albumin circulates through brain capillaries and releases FAs (56). In addition, FAs are released inside brain cells by deesterification from the *sn*-2 position of phospholipids, as catalyzed by phospholipase A_2 (PLA_2) (57). FAs released by PLA_2 are mainly PUFAs, whereas the FAs delivered by albumin reflect the wide variety of dietary FAs. Two PUFAs that are especially abundant in the brain, arachidonic acid and DHA, are thus released continuously from membrane phospholipids by PLA_2 activity. The PUFAs so generated remain localized mainly in the membrane, where they are ~50% ionized, hence increasing the net negative charge of the membrane surface (58). Therefore, their presence could initiate or enhance the binding of αS to the membrane.

Despite the fact that the physiological function of αS is still unknown, all available data suggest that the active protein form is represented by structured αS monomers or oligomers, which are adsorbed to lipid surfaces. If the altered FA metabolism in the presence of αS is in fact a result of the previously reported reduction in FA uptake

(29, 30), it may be concluded that the membrane-attached αS molecules affect the trafficking of FAs across the membrane, possibly by altering the equilibrium distribution of FAs in the leaflets of the lipid bilayer. This could occur (speculatively) either by diminishing the usually fast rates of FA flip-flop across the bilayer (59) or by influencing other membrane-bound proteins that allegedly act as FA transporters across the membrane (60). Conversely, if the reported lower FA uptake is induced by changes in FA turnover, it can be hypothesized that αS affects the corresponding enzymes that regulate FA storage and/or utilization inside the cell. In any case, the mechanisms underlying these effects need to be elucidated for a better understanding of the role that αS plays in the healthy brain.

This work was supported by National Institutes of Health Grant HI-26335 to J.A.H. The authors are indebted to Ronit Sharon, Ifat Bar-Joseph, and Dennis Selkoe (Brigham and Women's Hospital, Boston, MA) for providing purified αS and Fig. 4 as well as for helpful discussions. The authors also thank Jon Vural (Boston University School of Medicine) for technical assistance.

REFERENCES

1. Iwai, A., E. Masliah, M. Yoshimoto, N. Ge, L. Flanagan, H. A. de Silva, A. Kittel, and T. Saitoh. 1995. The precursor protein of non-Aβ component of Alzheimer's disease amyloid is a presynaptic protein of the central nervous system. *Neuron.* **14:** 467–475.
2. George, J. M., H. Jin, W. S. Woods, and D. F. Clayton. 1995. Characterization of a novel protein regulated during the critical period for song learning in the zebra finch. *Neuron.* **15:** 361–372.
3. Hashimoto, M., and E. Masliah. 1999. Alpha-synuclein in Lewy body disease and Alzheimer's disease. *Brain Pathol.* **9:** 707–720.
4. Polymeropoulos, M. H., C. Lavedan, E. Leroy, S. E. Ide, A. Dehejia, A. Dutra, B. Pike, H. Root, J. Rubenstein, R. Boyer, et al. 1997. Mutation in the α-synuclein gene identified in families with Parkinson's disease. *Science.* **276:** 2045–2047.
5. Krüger, R., W. Kuhn, T. Müller, D. Woitalla, M. Graeber, S. Kösel, H. Przuntek, J. T. Epplen, L. Schöls, and O. Riess. 1998. Ala30Pro mutation in the gene encoding α-synuclein in Parkinson's disease. *Nat. Genet.* **2:** 106–108.
6. Zarranz, J. J., J. Alegre, J. C. Gomez-Esteban, E. Lezcano, R. Ros, I. Ampuero, L. Vidal, J. Hoenicka, O. Rodriguez, B. Atares, et al. 2004. The new mutation, E46K, of α-synuclein causes Parkinson and Lewy body dementia. *Ann. Neurol.* **55:** 164–173.
7. Singleton, A. B., M. Farrer, J. Johnson, A. Singleton, S. Hague, J. Kachergus, M. Hulihan, T. Peuralinna, A. Dutra, R. Nussbaum, et al. 2003. α-Synuclein locus triplication causes Parkinson's disease. *Science.* **302:** 841.
8. Farrer, M., J. Kachergus, L. Forno, S. Lincoln, D. S. Wang, M. Hulihan, D. Maraganore, K. Gwinn-Hardy, Z. Wszolek, D. Dickson, et al. 2004. Comparison of kindreds with parkinsonism and α-synuclein genomic multiplications. *Ann. Neurol.* **55:** 174–179.
9. Clayton, D. F., and J. M. George. 1999. Synucleins in synaptic plasticity and neurodegenerative disorders. *J. Neurosci. Res.* **58:** 120–129.
10. Selkoe, D. J. 2003. Folding proteins in fatal ways. *Nature.* **426:** 900–904.
11. Conway, K. A., J. D. Harper, and P. T. Lansbury, Jr. 2000. Fibrils formed in vitro from α-synuclein and two mutant forms linked to Parkinson's disease are typical amyloid. *Biochemistry.* **39:** 2552–2563.
12. Ueda, K., H. Fukushima, E. Masliah, Y. Xia, A. Iwai, M. Yoshimoto, D. A. Otero, J. Kondo, Y. Ihara, and T. Saitoh. 1993. Molecular cloning of cDNA encoding an unrecognized component of amyloid in Alzheimer disease. *Proc. Natl. Acad. Sci. USA.* **90:** 11282–11286.
13. Volles, M. J., and P. T. Lansbury, Jr. 2003. Zeroing in on the pathogenic form of α-synuclein and its mechanism of neurotoxicity in Parkinson's disease. *Biochemistry.* **42:** 7871–7878.
14. Volles, M. J., S. J. Lee, J. C. Rochet, M. D. Shtilerman, T. T. Ding, J. C. Kessler, and P. T. Lansbury, Jr. 2001. Vesicle permeabilization by protofibrillar α-synuclein: implications for the pathogenesis and treatment of Parkinson's disease. *Biochemistry.* **40:** 7812–7819.
15. Walsh, D. M., I. Klyubin, J. V. Fadeeva, W. K. Cullen, R. Anwyl, M. S. Wolfe, M. J. Rowan, and D. J. Selkoe. 2002. Naturally secreted oligomers of amyloid β protein potently inhibit hippocampal long-term potentiation *in vivo*. *Nature.* **416:** 535–539.
16. Weinreb, P. H., W. Zhen, A. W. Poon, K. A. Conway, and P. T. Lansbury, Jr. 1996. NACP, a protein implicated in Alzheimer's disease and learning, is natively unfolded. *Biochemistry.* **35:** 13709–13715.
17. Davidson, W. S., A. Jonas, D. F. Clayton, and J. M. George. 1998. Stabilization of α-synuclein secondary structure upon binding to synthetic membranes. *J. Biol. Chem.* **273:** 9443–9449.
18. Eliezer, D., E. Kutluay, R. Bussell, Jr., and G. Browne. 2001. Conformational properties of α-synuclein in its free and lipid-associated states. *J. Mol. Biol.* **307:** 1061–1073.
19. Ramakrishnan, M., P. H. Jensen, and D. Marsh. 2003. α-Synuclein association with phosphatidylglycerol probed by lipid spin labels. *Biochemistry.* **42:** 12919–12926.
20. Jo, E., J. McLaurin, C. M. Yip, P. St. George-Hyslop, and P. E. Fraser. 2000. α-Synuclein membrane interactions and lipid specificity. *J. Biol. Chem.* **275:** 34328–34334.
21. Perrin, R. J., W. S. Woods, D. F. Clayton, and J. M. George. 2001. Exposure to long chain polyunsaturated fatty acids triggers rapid multimerization of synucleins. *J. Biol. Chem.* **276:** 41958–41962.
22. Kubo, S., V. M. Nemani, R. J. Chalkley, M. D. Anthony, N. Hattori, Y. Mizuno, R. H. Edwards, and D. L. Fortin. 2005. A combinatorial code for the interaction of α-synuclein with membranes. *J. Biol. Chem.* **280:** 31664–31672.
23. Nuscher, B., F. Kamp, T. Mehnert, S. Odoy, C. Haass, P. J. Kahle, and K. Beyer. 2004. α-Synuclein has a high affinity for packing defects in a bilayer membrane. A thermodynamics study. *J. Biol. Chem.* **279:** 21966–21975.
24. Trostchansky, A., S. Lind, R. Hodara, T. Oe, I. A. Blair, H. Ischiropoulos, H. Rubbo, and J. M. Souza. 2006. Interaction with phospholipids modulates α-synuclein nitration and lipid-protein adduct formation. *Biochem. J.* **393:** 343–349.
25. Sharon, R., M. S. Goldberg, I. Bar-Josef, R. A. Betensky, J. Shen, and D. J. Selkoe. 2001. α-Synuclein occurs in lipid-rich high-molecular-weight complexes, binds fatty acids, and shows homology to the fatty acid-binding proteins. *Proc. Natl. Acad. Sci. USA.* **98:** 9110–9115.
26. Sharon, R., I. Bar-Joseph, M. P. Frosch, D. M. Walsh, J. A. Hamilton, and D. J. Selkoe. 2003. The formation of highly soluble oligomers of α-synuclein is regulated by fatty acids and enhanced in Parkinson's disease. *Neuron.* **37:** 583–595.
27. Sharon, R., I. Bar-Joseph, G. E. Mirick, C. N. Serhan, and D. J. Selkoe. 2003. Altered fatty acid composition of dopaminergic neurons expressing α-synuclein and human brains with α-synucleinopathies. *J. Biol. Chem.* **278:** 49874–49881.
28. Lücke, C., L. H. Gutiérrez-González, and J. A. Hamilton. 2003. Intracellular lipid binding proteins: evolution, structure and ligand binding. *In* Cellular Proteins and Their Fatty Acids in Health and Disease. A. K. Duttaroy and F. Spener, editors. Wiley-VCH, Weinheim, Germany. 95–118.
29. Golovko, M. Y., N. J. Faergeman, N. B. Cole, P. I. Castagnet, R. L. Nussbaum, and E. J. Murphy. 2005. α-Synuclein gene deletion decreases brain palmitate uptake and alters the palmitate metabolism in the absence of α-synuclein palmitate binding. *Biochemistry.* **44:** 8251–8259.
30. Castagnet, P. I., M. Y. Golovko, G. C. Barceló-Coblijn, R. L. Nussbaum, and E. J. Murphy. 2005. Fatty acid incorporation is decreased in astrocytes cultured from α-synuclein gene-ablated mice. *J. Neurochem.* **94:** 839–849.
31. Hamilton, J. A. 2004. Fatty acid interactions with proteins: what X-ray crystal and NMR solution structures tell us. *Prog. Lipid Res.* **43:** 177–199.
32. Kirk, W. R., E. Kurian, and F. G. Prendergast. 1996. Characterization of the sources of protein-ligand affinity: 1-sulfonato-8-(1′)anilinonaphthalene binding to intestinal fatty acid binding protein. *Biophys. J.* **70:** 69–83.
33. Conway, K. A., J. D. Harper, and P. T. Lansbury. 1998. Accelerated *in vitro* fibril formation by a mutant α-synuclein linked to early-onset Parkinson disease. *Nat. Med.* **4:** 1318–1320.
34. Cistola, D. P., D. M. Small, and J. A. Hamilton. 1987. Carbon 13 NMR studies of saturated fatty acids bound to bovine serum al-

bumin. I. The filling of individual fatty acid binding sites. *J. Biol. Chem.* **262:** 10971–10979.
35. Harris, J. R., and R. W. Horne. 1991. Negative staining. *In* Electron Microscopy in Biology. J. R. Harris, editor. IRL Press, Oxford, UK. 203–228.
36. Dubochet, J., M. Groom, and S. Mueller-Neuteboom. 1982. The mounting of macromolecules for electron microscopy with particular reference to surface phenomena and the treatment of support films by glow discharge. *Adv. Opt. Electron Microsc.* **8:** 107–135.
37. Lücke, C., F. Zhang, H. Rüterjans, J. A. Hamilton, and J. C. Sacchettini. 1996. Flexibility is a likely determinant of binding specificity in the case of ileal lipid binding protein. *Structure.* **4:** 785–800.
38. Zhang, F., C. Lücke, L. J. Baier, J. C. Sacchettini, and J. A. Hamilton. 1997. Solution structure of human intestinal fatty acid binding protein: implications for ligand entry and exit. *J. Biomol. NMR.* **9:** 213–228.
39. Zhang, F., C. Lücke, L. J. Baier, J. C. Sacchettini, and J. A. Hamilton. 2003. Solution structure of human intestinal fatty acid binding protein with a naturally-occurring single amino acid substitution (A54T) that is associated with altered lipid metabolism. *Biochemistry.* **42:** 7339–7347.
40. Wishart, D. S., B. D. Sykes, and F. M. Richards. 1991. Simple techniques for the quantification of protein secondary structure by ^{1}H NMR spectroscopy. *FEBS Lett.* **293:** 72–80.
41. Cistola, D. P., M. T. Walsh, R. P. Corey, J. A. Hamilton, and P. Brecher. 1988. Interactions of oleic acid with liver fatty acid binding protein: a carbon-13 NMR study. *Biochemistry.* **27:** 711–717.
42. Parks, J. S., D. P. Cistola, D. M. Small, and J. A. Hamilton. 1983. Interactions of the carboxyl group of oleic acid with bovine serum albumin: a ^{13}C NMR study. *J. Biol. Chem.* **258:** 9262–9269.
43. Hamilton, J. A., D. P. Cistola, J. D. Morrisett, J. T. Sparrow, and D. M. Small. 1984. Interactions of myristic acid with bovine serum albumin: a ^{13}C NMR study. *Proc. Natl. Acad. Sci. USA.* **81:** 3718–3722.
44. Cistola, D. P., J. C. Sacchettini, L. J. Banaszak, M. T. Walsh, and J. I. Gordon. 1989. Fatty acid interactions with rat intestinal and liver fatty acid-binding proteins expressed in *Escherichia coli.* A comparative ^{13}C NMR study. *J. Biol. Chem.* **264:** 2700–2710.
45. Cistola, D. P., J. A. Hamilton, D. Jackson, and D. M. Small. 1988. Ionization and phase behavior of fatty acids in water: application of the Gibbs phase rule. *Biochemistry.* **27:** 1881–1888.
46. Hamilton, J. A., and F. Kamp. 1999. How are free fatty acids transported in membranes? Is it by proteins or by free diffusion through the lipids? *Diabetes.* **48:** 2255–2269.
47. Spooner, P. J. R., S. B. Clark, D. L. Gantz, J. A. Hamilton, and D. M. Small. 1988. The ionization and distribution behavior of oleic acid in chylomicrons and chylomicron-like emulsion particles and the influence of serum albumin. *J. Biol. Chem.* **263:** 1444–1453.
48. Zhu, M., J. Li, and A. L. Fink. 2003. The association of α-synuclein with membranes affects bilayer structure, stability, and fibril formation. *J. Biol. Chem.* **278:** 40186–40197.
49. Bussell, R., Jr., and D. Eliezer. 2003. A structural and functional role for 11-mer repeats in α-synuclein and other exchangeable lipid binding proteins. *J. Mol. Biol.* **329:** 763–778.
50. Chandra, S., X. Chen, J. Rizo, R. Jahn, and T. C. Südhof. 2003. A broken α-helix in folded α-synuclein. *J. Biol. Chem.* **278:** 15313–15318.
51. Bussell, R., Jr., T. F. Ramlall, and D. Eliezer. 2005. Helix periodicity, topology, and dynamics of membrane-associated α-synuclein. *Protein Sci.* **14:** 862–872.
52. Cistola, D. P., D. Atkinson, J. A. Hamilton, and D. M. Small. 1986. Phase behavior and bilayer properties of fatty acids: hydrated 1:1 acid-soaps. *Biochemistry.* **25:** 2804–2812.
53. Chen, I. A., and J. W. Szostak. 2004. A kinetic study of the growth of fatty acid vesicles. *Biophys. J.* **87:** 988–998.
54. Gawrisch, K., N. V. Eldho, and L. L. Holte. 2003. The structure of DHA in phospholipid membranes. *Lipids.* **38:** 445–452.
55. Moser, H. W. 1997. Adrenoleukodystrophy: phenotype, genetics, pathogenesis and therapy. *Brain.* **120:** 1485–1508.
56. Rapoport, S. I., M. C. J. Chang, and A. A. Spector. 2001. Delivery and turnover of plasma-derived essential PUFAs in mammalian brain. *J. Lipid Res.* **42:** 678–685.
57. Rapoport, S. I. 2001. In vivo fatty acid incorporation into brain phospholipids in relation to plasma availability, signal transduction and membrane remodeling. *J. Mol. Neurosci.* **16:** 243–262.
58. Hamilton, J. A. 1995. ^{13}C NMR studies of the interaction of fatty acids with phospholipid bilayers, plasma lipoproteins, and proteins. *In* Carbon-13 Magnetic Resonance Spectroscopy of Biological Systems. N. Beckmann, editor. Academic Press, San Diego, CA. 117–155.
59. Kamp, F., and J. A. Hamilton. 1992. pH gradients across phospholipid membranes caused by fast flip-flop of fatty acids. *Proc. Natl. Acad. Sci. USA.* **85:** 11367–11370.
60. Abumrad, N., C. Harmon, and A. Ibrahimi. 1998. Membrane transport of long-chain fatty acids: evidence for a facilitated process. *J. Lipid Res.* **39:** 2309–2318.